Metabolic Engineering Communications 10 (2020) e00117

Contents lists available at ScienceDirect

Metabolic Engineering Communications

journal homepage: www.elsevier.com/locate/mec

Improving heterologous protein expression in *Synechocystis* sp. PCC 6803 for alpha-bisabolene production

Jacob Sebesta [a], Christie AM. Peebles [a,b,*]

[a] Department of Chemical and Biological Engineering, Colorado State University, Fort Collins, CO, 80523, USA
[b] Department of Cell and Molecular Biology, Colorado State University, Fort Collins, CO, 80523, USA

ARTICLE INFO

Keywords:
Synechocystis sp. PCC6803
Bisabolene
Ribosome binding site
Metabolic engineering
Synthetic biology

ABSTRACT

Cyanobacterial biofuels have the potential to reduce the cost and climate impacts of biofuel production because primary carbon fixation and conversion to fuel are completed together in the cultivation of the cyanobacteria. Cyanobacterial biofuels, therefore, do not rely on costly organic carbon feedstocks that heterotrophs require, which reduces competition for agricultural resources such as arable land and freshwater. However, the published product titer achieved for most molecules of interest using cyanobacteria lag behind what has been achieved using yeast and *Escherichia coli* (*E. coli*) cultures. In *Synechocystis* sp. PCC 6803 (*S.* 6803), we attempted to increase the product titer of the sesquiterpene, bisabolene, which may be converted to bisabolane, a possible diesel replacement. We tested 19 strains of genetically modified *S.* 6803 with five different codon usage sequences of the bisabolene synthase from the grand fir tree (*Abies grandis*). At least three ribosome binding sites (most designed using the RBS Calculator) were tested for each codon usage sequence. We also tested strains with and without the farnesyl pyrophosphate synthase gene from *E. coli*. Bisabolene titers after five days of growth in continuous light ranged from un-detected to 7.8 mg/L. Bisabolene synthase abundance was measured and found to be well correlated with titer. Select strains were also tested in 12:12 light:dark cycles, where similar titers were reached after the same amount of light exposure time. One engineered strain was also tested in photobioreactors exposed to a simulated outdoor light pattern with maximum light intensity of 1600 μmol photons m^{-2} s^{-1}. Here, the bisabolene titer reached 22.2 mg/L after 36 days of growth. Dramatic improvements in our ability to control gene expression in cyanobacteria such as *S.* 6803, and the co-utilization of additional metabolic engineering methods, are needed in order for these titers to improve to the levels reported for engineered *E. coli*.

1. Background

Development of biofuel production technology offers one potential path for generating renewable energy that could reduce the rate of increase of concentrations of atmospheric greenhouse gases generated from human activity. Metabolic engineering of photoautotrophs such as cyanobacteria and microalgae offers the potential to design processes that directly convert sunlight into biofuel products or precursors. This avoids the necessity of growing crops for carbohydrate feedstocks required for heterotrophic cultivation as is currently implemented in the microbial conversion of maize to biofuels. Cyanobacteria and microalgae have higher areal biomass productivities than land crops and do not require arable land (Dismukes et al., 2008). A comparison of microalgal biodiesel to soybean biodiesel has also shown the net energy ratio (energy consumed by all processing steps divided by the energy produced) to be more favorable in microalgal biodiesel (Batan et al., 2010).

Though cyanobacteria generally also grow more slowly than heterotrophs, some species such as *Synechococcus* UTEX 2973 approach the growth rate of *Saccharomyces cerevisiae*, with a doubling time of 1.9 hours (Yu et al., 2015). Many species of cyanobacteria are salt tolerant, allowing their growth in seawater (Pade and Hagemann, 2014), and municipal wastewater streams have also been proposed as media that provide nitrogen and phosphorous (Gonçalves et al., 2016; Hughes et al., 2018). The advantages of these species may be eventually realized by translating what is learned from our current model cyanobacteria for use with those species. *Synechocystis* sp. PCC 6803 (*S.* 6803) is a model cyanobacteria and has been widely studied from the perspectives of metabolic engineering and of photoautotroph biology. The chromosome of *S.* 6803 can be easily modified using the organism's native homologous recombination mechanisms. In addition, several replicative

* Corresponding author. Department of Chemical and Biological Engineering, Colorado State University, Fort Collins, CO, 80523, USA.
E-mail address: christie.peebles@colostate.edu (C.AM. Peebles).

https://doi.org/10.1016/j.mec.2019.e00117
Received 24 July 2019; Received in revised form 10 November 2019; Accepted 3 December 2019

plasmids have been used to modify *S.* 6803 without modifying the chromosome (Ferreira et al., 2018; Huang et al., 2010; Jin et al., 2018; Liu and Pakrasi, 2018). The genome of *S.* 6803 was sequenced in 1996 (Kaneko et al., 1996), and other genome projects listed on the CyanoBase website (http://genome.microbedb.jp/CyanoBase) have reached 376 cyanobacterial species.

A robust research community is engaged in developing and testing diverse genetic parts and studying the biology of cyanobacteria. Many genes from different organisms have been expressed heterologously in cyanobacteria. The genetic elements necessary for expressing these proteins, including promoters and ribosome binding sites (RBSs), have been directly adapted from use in *Escherichia coli* (*E. coli)* or have been elements copied from the cyanobacteria species itself (Huang and Lindblad, 2013; Wang et al., 2018). The RBS Calculator has also been applied for the development of those genetic parts in cyanobacteria (Markley et al., 2015). A recent review (Carroll et al., 2018) covers these topics in detail, including the advancements achieved in metabolic engineering of cyanobacteria in terms of the titers achieved for many products.

One class of molecules, terpenoids, have been targeted for production in cyanobacteria which may be utilized in industries ranging from pharmaceuticals, to commodity chemicals and fuels. One successful example of metabolic engineering in cyanobacteria is provided by Gao et al., who achieved a product titer of 1.26 g/L of the five-carbon terpenoid, isoprene in *Synechococcus elongatus* by implementing many common metabolic engineering strategies in combination (Gao et al., 2016). Similar product titers have not been achieved for more complex terpenoids. For example, the C10 monoterpene, limonene, has been produced at titers of 1 mg/L after 30 days of cultivation (Kiyota et al., 2014), and 6.7 mg/L after 7 days (Lin et al., 2017). The C15 sesquiterpene, caryophyllene, was produced at a titer of 46 μg/L after seven days (Reinsvold et al., 2011). Pattanaik and Lindberg have provided a review of terpenoid production in cyanobacteria (Pattanaik and Lindberg, 2015).

Davies et al. previously engineered *Synechococcus* sp. PCC 7002 to produce 0.6 mg/L bisabolene by expressing a codon optimized sequence bisabolene synthase from *Abies grandis (A. grandis),* using the strong, constitutive cpcBA promoter from *S.* 6803 (Davies et al., 2014). In this work we increased bisabolene production in *S.* 6803 by varying codon usage and RBS sequences to control expression of bisabolene synthase. We utilized a counterselection method (Cheah et al., 2013) and inducible promoter (Albers et al., 2015) previously developed in our lab. Five codon optimizations of the bisabolene synthase gene from *A. grandis* were compared and, for each codon optimization, three or four RBS sequences designed by the RBS Calculator (Salis et al., 2009) were utilized. The co-expression of farnesyl pyrophosphate synthase from *E. coli* was also hypothesized to increase the supply of the substrate molecule for bisabolene synthase and therefore increase the bisabolene titer. Here, we present the impact these variations in genetic sequences had on bisabolene synthase expression and on bisabolene production.

2. Methods

2.1. Strains and cultivation

S. 6803 seed cultures were started from freezer stocks (5% DMSO, stored at −80 °C) and, generally, were grown in shake flasks containing 45 mL BG-11 media (Stanier et al., 1979) with phosphate increased to 1 mM, and buffered with 10 mM TES-NaOH, pH 8.0. All strains were grown at 30 °C under fluorescent light at approximately 200 ± 20 μmol photons/m^2/s with shaking at 200 rpm. Optical density was monitored by measuring absorbance at 730 nm using a NanoDrop spectrophotometer (ThermoFisher Scientific). For continuous light experiments, 0.9 mL of 1 M sodium bicarbonate was added every 12 h of growth starting at 0 h. For 12 h:12 h light:dark cycles, in which the lights were turned off while shaking continued, 0.9 mL of 1 M sodium bicarbonate was added every 24 h, at the beginning of the light period. Bisabolene synthase (and when the gene was also present, farnesyl pyrophosphate synthase) expression was induced by addition of IPTG to 1 mM at 12 h after inoculation, and 9 mL of dodecane (Sigma-Aldrich) was added directly to flasks at the time of induction.

Photobioreactor experiments were completed using 3 L photobioreactors (Allen Scientific Glass, Boulder, CO, USA) containing 1.5 L BG-11 (with 1 mM phosphate) buffered with 10 mM TES-NaOH, pH 8.0. An air stream enriched to 5% CO_2 was supplied to the bottom of the reactor at a rate of 200 mL min^{-1}, following the reactor setup and operation described by Werner et al. (2019). However, in this case, the cultures were not entrained to the light:dark cycle before commencing the experiment. We simulated outdoor sunlight exposure for the photobioreactors with two 4000k white LED panels (Reliance Laboratories, Port Townsend, WA, USA) programmed with a sinusoidal light intensity curve peaking at a light intensity of approximately 1600 μmol photons m^{-2} s^{-1}, with 12 h of darkness. The reactors were inoculated from shake flask cultures to an initial $OD_{730\ nm}$ of 2.0, which we found was necessary for the cultures to survive the high light intensity. A 150 mL dodecane overlay and IPTG to 1 mM were added to this at the time of inoculation of the PBRs.

E. coli (DH5α) was used for plasmid construction and was grown at 37 °C in lysogeny broth. Initial plasmids used for generating a markerless bisabolene synthase-expressing strain were assembled using ligase cycling reactions (Kok et al., 2014) (PCR of parts using New England Biolabs Phusion DNA polymerase, ligase cycling using Ampligase from Lucigen). Bisabolene synthase codon usage variants were synthesized by GenScript ('GS') and IDT ('IDT', 'EuH', and 'HCR') or PCR amplified from a plasmid ('2.0'), and inserted into plasmids using Gibson Assembly (Gibson et al., 2009). RBS variant plasmids were generated using ligase cycling. Correct colonies were screened via colony PCR, and then sequenced (GeneWiz or QuintaraBio). Transformation of WT *S.* 6803 was completed as previously described by Cheah et al. (2013). Colonies were screened by colony PCR, and the sequences were confirmed by Sanger sequencing reactions covering the 3' region of the upstream homologous region, the promoter, RBS, and the entire bisabolene synthase gene.

2.2. Bisabolene measurement (GC-MS)

Samples of dodecane were taken directly from dodecane layers of shake flask and photobioreactor cultures to measure the bisabolene concentration. These samples were analyzed on an Agilent 6893 GC equipped with an Agilent 5973N mass spectrometer. A 50 m Agilent HP-5 column was used to separate hydrophobic molecules. Oven temperature was ramped from 180 °C to 260 °C at a rate of 15 °C/min. Bisabolene quantities were calculated based on a standard curve generated using serial dilutions of bisabolene (mixture of isomers, AlfaAesar). The software, Automated Mass spectral Deconvolution and Identification System (AMDIS), was used to analyze the spectral data and identify bisabolene (chemdata.nist.gov).

2.3. Protein abundance (Western blot)

Cultures of each strain were grown for 48 h, starting at OD730 = 0.05, with induction by 1 mM IPTG added at 12 h, and no dodecane added. Cells were harvested by centrifugation, frozen in liquid nitrogen, and stored at −80 °C for less than three weeks. Frozen cell pellets were thawed on ice and resuspended with 0.5 mL ice cold PBS, pH 7.4. These were centrifuged and the supernatant fully removed before being resuspended in 500 μL lysis buffer consisting of 1x PBS, pH 7.4, 0.1% Triton X-100, 1 mM DTT, and 1x HALT protease inhibitor (ThermoScientific). Cells were lysed by sonication (Misonix model S-4000, with a microtip, at 45% power, 3s on/3s off for 2 min processing time), and the cell debris removed by centrifugation (12,000 x g for 10 min). The total protein concentration in the lysate was measured using a Pierce BCA Protein Assay kit and a BMG FLUOstar Omega microplate reader. For each bioreplicate, 25 μg of total protein was loaded into a lane of a

BioRad MiniPROTEAN TGX pre-cast gel. A relative standard curve was included on each gel which consisted of the pooled lysate from three 50 mL flasks of the 2.0–10xB strain grown using the same methods as used to obtain protein samples from the other strains. Four different amounts of this lysate were loaded in four lanes of each gel to generate a relative response curve. Proteins were transferred from the gel to PVDF membrane at 100 V for 100 min on ice in 1x TRIS/Glycine/SDS, and 20% methanol. Membranes were blocked overnight at 4 °C in PBS, 0.05% Tween20, 5 mM EDTA, and 5% nonfat milk with gentle shaking. Mouse anti-histag antibody (ThermoFisher Scientific) was diluted 1:2500 in 1x PBS, 0.05% Tween20, 0.5% nonfat milk, and 5 mM EDTA, and the membrane was incubated in the primary antibody solution with gentle shaking for 2 h at room temperature. The membranes were then washed in PBS with 0.05% Tween20 once for 15 min and then twice for 5 min each before being incubated in a 1:25,000 dilution of goat anti-mouse antibody conjugated to horseradish peroxidase (ThermoFisher Scientific) (in 1x PBS, 0.05% Tween20, and 0.5% nonfat milk) for 2 h with gentle shaking at room temperature. Again, the membranes were then washed in PBS 0.05% Tween20 once for 15 min and then twice for 5 min each before being incubated at room temperature for 5 min with 500 μL of SuperSignal West Femto Maximum Sensitivity ECL substrate (Thermo Scientific) between sheets of plastic wrap. Membranes were imaged using a UVP BioChemi gel imager and band intensity was quantified using ImageJ software (Schneider et al., 2012).

To quantify the fraction of total protein in the engineered strains represented by bisabolene synthase, immobilized metal affinity chromatography was utilized to purify bisabolene synthase. *E. coli* (DE3 strain lemo21, New England Biolabs) transformed with the plasmid expressing the GS100x construct was grown to OD600 of 1.2, at which point IPTG was added to 1 mM and the culture incubated with shaking at 22 °C for 24 h. Cells were centrifuged and the pellets frozen at −80 °C. Cells were resuspended in 1x PBS, pH 7.4, 0.1% Triton X-100, 1 mM DTT, and 1x HALT protease inhibitor, and sonicated to lyse the cells. BioRad Profinity IMAC resin was used to purify the histagged bisabolene synthase. The binding, wash, and elution buffers suggested by the Profinity manual were used.

3. Results

We initially designed a strain of *S.* 6803 to express the bisabolene synthase from *A. grandis* (Fig. 1), with the sequence codon optimized by GenScript for expression in *S.* 6803. This strain used the IPTG-inducible

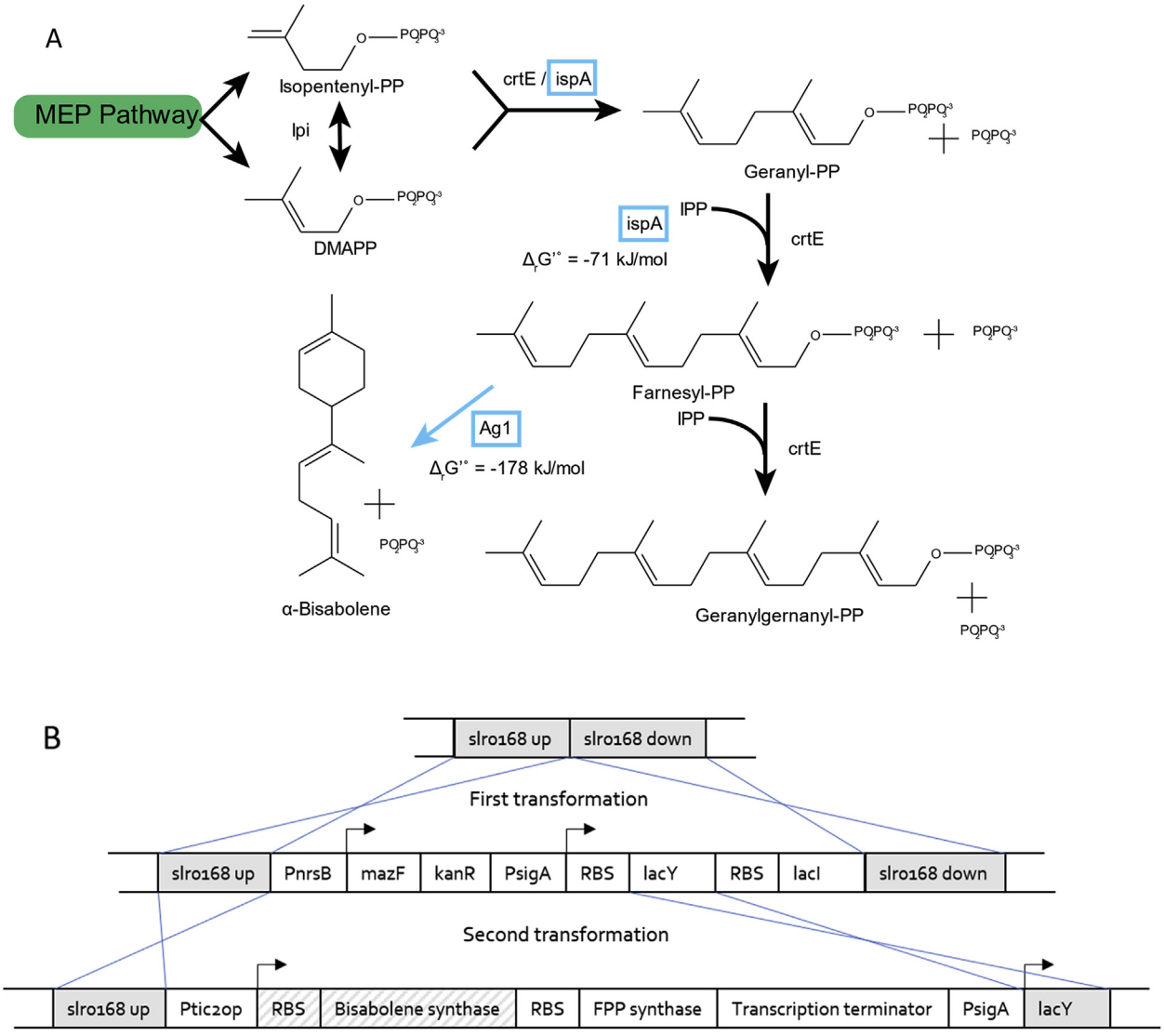

Fig. 1. Terpene synthesis in *S.* 6803 (A). Blue boxes indicate the heterologous genes used ispA gene from *E. coli* and the bisabolene synthase gene from *Abies grandis*. The two-step selection/counterselection transformation allows the generation of strains without selection markers (B). (For interpretation of the references to colour in this figure legend, the reader is referred to the Web version of this article.)

Ptic2op promoter and the RBS inherited from that promoter (Albers et al., 2015). After five days of growth in shake flasks under continuous light, this strain had produced 1.1 ± 0.08 mg/L bisabolene. According to the metabolic network of S. 6803 available in KEGG, the native terpenoid synthase pathway uses one enzyme to catalyze the production of geranyl pyrophosphate, farnesyl pyrophosphate and geranylgeranyl pyrophosphate. We hypothesized that this may result in low concentrations of farnesyl pyrophosphate in the cell, and that co-expression of a farnesyl pyrophosphate synthase may increase the production of bisabolene.

We cloned the farnesyl pyrophosphate synthase from *E. coli,* codon optimized by GenScript, into an operon downstream of the bisabolene synthase gene. Denoted 'GS1x', this engineered strain produced bisabolene at 1.6 ± 0.2 mg/L when grown in 45 mL BG-11 in shake flasks for five days. Since the strain that expressed both genes had a significantly higher bisabolene titer, we included farnesyl pyrophosphate synthase in all future strains. To further increase the product titer of bisabolene, we attempted to increase the expression of bisabolene synthase in *S.* 6803 by testing different codon optimized sequences and RBS sequences. In these designs, Ptic2op initiated transcription (when induced by addition of IPTG) of a bicistronic operon including a GenScript codon optimized sequences for *A. grandis* bisabolene synthase and farnesyl pyrophosphate synthase from *E. coli*. This sequence, along with constitutively expressed lacY and lacI for Ptic2op induction/repression, was integrated into the slr0168 neutral site containing the *mazF* counterselection cassette (Cheah et al., 2013). This cassette replaced the nickel-inducible counter-selection marker *(mazF)* and the kanamycin resistance gene, such that no selection marker was present in the final strain. No growth defects were observed due to either the presence of a dodecane layer or due to the expression of bisabolene synthase and farnesyl pyrophosphate synthase (see Supplementary Fig. 1). During the exponential growth phase, the specific growth rates were all between 0.09 and 0.11 hr^{-1}, corresponding to a doubling time between 7.3 h and 6.1 h.

3.1. Codon optimization

Five codon optimization strategies were tested (the sequences are given in Table S2). The GenScript optimization of bisabolene synthase was described above, denoted 'GS.' IDT (Integrated DNA Technologies) codon optimization tool was utilized to optimize the bisabolene synthase gene, denoted 'IDT,' for *S.* 6803. A bisabolene synthase gene optimized by DNA2.0 for expression in *Synechococcus p.* PCC 7002 was provided as a gift from Dr. Fiona Davies (Davies et al., 2014). Strains using this sequence are denoted '2.0'. The free software, EuGene, was utilized to design two additional codon optimizations (Gaspar et al., 2012). One utilized only the harmonization algorithm, denoted 'EuH', which considers the codon usage frequency of the native host organism and attempts to match that frequency in the design for the target organism. This function was likely impaired by a lack of published gene sequences from *A. grandis*. Only 16 gene sequences were available from the Dendrome Project (now available at treegenesdb.org) to calculate codon usage for the native organism. Another sequence, denoted 'EuHCR', utilized the harmonization, codon context, and remove repeats rules.

The five sequences have between 73% and 80% sequence identity. The codon adaptation index (CAI) compares the codon usage of a given gene sequence to the codon usage frequency of the organism (Sharp and Li, 1987). The GenScript optimization had the highest CAI at 0.89, while the DNA2.0, IDT, and EuH each had CAI between 0.76 and 0.71. The EuHCR-optimized gene had a CAI of 0.64. We measured the bisabolene titer of five strains of *S.* 6803 expressing each of the codon optimizations using identical promoters (Ptic2op) and the RBS inherent to the that promoter. After five days of growth in continuous light, the bisabolene titer of these strains varied from 0.1 ± 0.2 mg/L for the EuHCR strain to 1.6 ± 0.2 mg/L for the GenScript-optimized strain (see Fig. 2). The EuH, DNA2.0, and IDT optimized strains, which had similar CAI, also had similar bisabolene titers of 1.0 ± 0.2, 0.8 ± 0.2, and 0.7 ± 0.1 mg/L, respectively. Bisabolene titer and CAI were well correlated with an R^2 value of 0.85 determined for the linear regression.

3.2. Ribosome binding site design

RBSs were designed using the RBS Calculator (Espah Borujeni et al., 2014, 2017; Espah Borujeni and Salis, 2016; Salis et al., 2009) forward engineering tool (free energy version v1.1) using the pre-sequence 'GATAACAATT' corresponding to the sequence of the Ptic2op promoter just 5′ of the RBS and transcription start site. The first 30 nucleotides of codon optimized bisabolene synthase sequence were entered as the gene sequence (see Table 1). Two RBSs were designed for each codon optimized gene sequence with a target expression level of 2000 (arbitrary units), or about ten times the expression level predicted by the RBS Calculator for the GS1x strain. After we constructed strains based on these designs, the RBS Calculator was revised (free energy version v2.1), and we recalculated predicted expression levels using the updated calculator. The translation initiation rates predicted by both versions of the calculator for each RBS used in this study are provided in Supplementary Table S1.

Utilizing different RBSs for each codon optimization allowed us to reach a bisabolene titer of 7.9 ± 0.6 mg/L for one strain (2.0–10xB), though most strains generated titers between 0.4 and 2.7 mg/L, and the

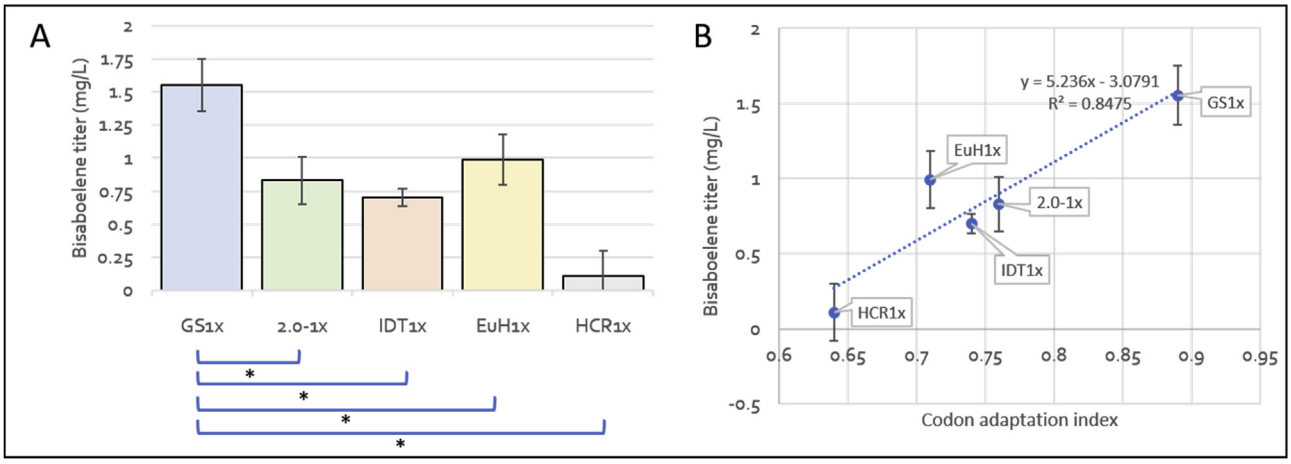

Fig. 2. Comparison of bisabolene titer for five different codon optimizations of bisabolene synthase (A), and the codon adaptation index for each of these strains versus bisabolene titer (B). Error bars indicate the standard deviation of the titer measured from three biological replicates with two GC-MS technical replicates each. Asterisks indicate significant differences between a designed RBS sequence and the base case for that codon optimization with (paired *t*-test with $p < 0.05$).

Table 1
RBS sequences used in this work. The preceding sequence and the first 30 nucleotides of the gene used to design the RBSs in RBS Calculator are also shown.

Strain	RBS sequence	Gene sequence (first 30 nt)
Pre-sequence: AATTGTGAGCGGATAACAATT		
GS1x	TCACACAGGAAACAGAATCAT	ATGGCTGGAGTGTCTGCCGTGAGCAAAGTG
GS10xA	AAACCTACGTAAACCCCTTTTTAAGGTAAAAG	ATGGCTGGAGTGTCTGCCGTGAGCAAAGTG
GS10xB	ACCAACACCTTTTAGAAGGGGTAAATTATA	ATGGCTGGAGTGTCTGCCGTGAGCAAAGTG
GS100x	ATCCCCCAAACCAAAGGGAGGTTTAAGA	ATGGCTGGAGTGTCTGCCGTGAGCAAAGTG
2.0–1x	TCACACAGGAAACAGAATCAT	ATGGCCGGTGTGAGCGCAGTGAGTAAAGTG
2.0–10xA	GAGGAGACGGACCCTTTCCAAGACGTTTAGGTAAG	ATGGCCGGTGTGAGCGCAGTGAGTAAAGTG
2.0–10xB	TTATTCTAAAATCTAACTATTATAGGAAGAGATT	ATGGCCGGTGTGAGCGCAGTGAGTAAAGTG
IDT1x	TCACACAGGAAACAGAATCAT	ATGGCTGGAGTCTCCGCGGTGAGTAAAGTT
IDT10xA	CAATAGCATCTATATAAAACATATCGGTAAAA	ATGGCTGGAGTCTCCGCGGTGAGTAAAGTT
IDT10xB	TCGGTAGCCGAAAAAAAATCCAAGTAGGTATCGAA	ATGGCTGGAGTCTCCGCGGTGAGTAAAGTT
EuH1x	TCACACAGGAAACAGAATCAT	ATGGCCGGAGTGAGTGCCGTCAGCAAGGTG
EuH10xA	AACAGGAATATACTATTTAGAGGTACGGTAAACAT	ATGGCCGGAGTGAGTGCCGTCAGCAAGGTG
EuH10xB	CACACAGAAAGGAGAAGTCAGAAAACAA	ATGGCCGGAGTGAGTGCCGTCAGCAAGGTG
HCR1x	TCACACAGGAAACAGAATCAT	ATGGCGGGGGTATCGGCGGTTTCCAAGGTT
HCR10xA	GCGCAGCACATCGCAACAATAAAAGGGCTAT	ATGGCGGGGGTATCGGCGGTTTCCAAGGTT
HCR10xB	TTCACAAAATTCTTTTAGTTTAGGCGTCAAC	ATGGCGGGGGTATCGGCGGTTTCCAAGGTT
Pre-sequence: CACCATCATCACCATTAATAA		
FPPS	CGAGGAAAACCAT	ATGGATTTTCCCCAACAACTGGAAGCCTGC

bisabolene concentration was below the detection limit in two cases (HCR10xA and HCR10xB) (see Fig. 3). Within each set of strains that used the same codon optimized bisabolene synthase, RBS sequences designed to have higher translation initiation rates either increased or decreased the bisabolene titer from the base case titer for that codon optimization. For example, one RBS sequence designed to have 10-fold higher expression than the base case GenScript codon optimization strain had a statistically similar titer, while the other actually had a lower titer of 0.9 ± 0.2 mg/L compared to 1.6 ± 0.2 mg/L. The strain with an RBS designed to have expression 100-fold higher than that for the same base case strain did achieve a higher bisabolene titer of 2.5 ± 0.4 mg/L. The two designed RBS for the EuHCR codon optimization resulted in

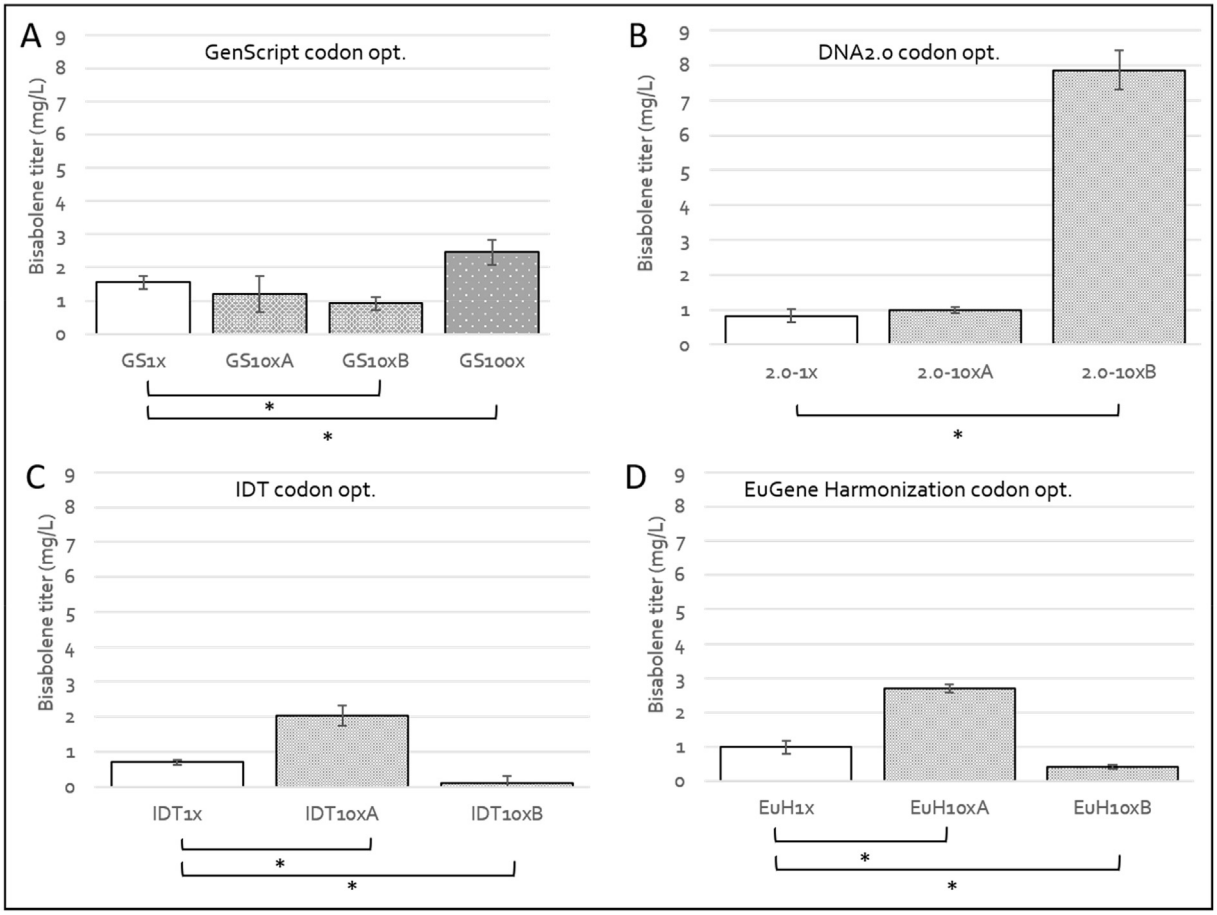

Fig. 3. Bisabolene titer for S. 6803 strains with RBS sequences designed for higher translation initiation rates for codon optimized gene sequence designed by GenScript (A), DNA2.0 for expression in *Synechococcus sp.* PCC7002 (B), IDT (C), and EuGene (D). Error bars indicate the standard deviation of the titer measured from three biological replicates with two GC-MS technical replicates each. Asterisks indicate significant differences between a designed RBS sequence and the base case for that codon optimization with (paired *t*-test with $p < 0.05$).

strains that failed to produce detectable levels of bisabolene (corresponding to a titer of 0.01 mg/L). The RBS Calculator-predicted expression level only poorly trended with bisabolene titer (Fig. 4b).

We compared the measured bisabolene titer to the relative bisabolene concentration for these strains using Western blotting to validate the assumption that bisabolene titer could be used as a proxy for gene expression. Bisabolene titer and relative bisabolene synthase concentration were well correlated (see Fig. 4). The relative bisabolene synthase concentration did not correlate as well with the RBS Calculator v2.1-predicted translation initiation rate, though this version did improve upon the previous version. A final Western blot containing a serial dilution of purified bisabolene synthase was used to estimate the fraction of total protein represented by bisabolene synthase in these samples. For the highest expressing strain, 2.0–10xB, bisabolene synthase was only 0.4 % of the total protein. The presence of bisabolene synthase and farnesyl pyrophosphate synthase in the 2.0–10xB strain was also verified using LC-MS/MS (data not shown).

3.3. Impact on light:dark cycle cultivation on bisabolene titer

Cheah et al. (2013) previously explored an important, but often overlooked, aspect of cyanobacterial metabolic engineering. Engineered strains are often tested in shake flasks under continuous light, though industrial cultivation is likely to occur outside and be subject to diurnal light fluctuations. They found that strains successfully engineered to produce higher titers of free fatty acids in continuous light lost all advantage over wild type cells with regards to titer when grown in 12:12 light-dark cycles. Since bisabolene is not produced by wild type *S.* 6803, we could only explore the impact of light-dark cycles on the mutant strains. Two strains, GS1x and 2.0–10xB, were grown in 12:12 light dark cycles for either 5 days or 10 days. When grown for 5 days in light-dark cycles, the titer of each was less than half of what it had been when grown for the same time period in continuous light (0.6 vs. 1.6 mg/L for GS1x and 2.6 vs 7.8 mg/L for 2.0–10xB, see Fig. 5). Growth in light-dark cycles for 10 days exposed the cultures to the same total amount of light as the 5-day continuous light cultures, and these cultures ended up with cell densities closer to the 5-day continuous light cultures than the 5-day light-dark cycle cultures. Both strains achieved higher titers of bisabolene (2.7 mg/L for GS1x and 9.7 mg/L for 2.0–10xB) when grown in 10-day light-dark cycles. The statistical significance of these comparisons is unclear when comparing on a specific titer basis. The specific titer of GS1x grown for 10-days in a light:dark cycle was higher than the 5-day continuous light culture, whereas, for 2.0–10xB, the 10-day light:dark cycle cultures had a similar titer to the cultures grown for 5-days in continuous light. Only for 2.0–10xB was the specific titer when grown in a 5-day light-dark cycle significantly different than when grown in a 5-day continuous light condition.

3.4. Bisabolene production in a photobioreactor

The best-performing strain, 2.0–10xB, was grown in a 3 L photobioreactor containing 1.5 L BG-11, aerated with 200 mL min^{-1} 5% CO_2-enriched air, following the reactor setup and operation described by Werner et al. (2019) including simulated outdoor sunlight exposure for the photobioreactors. After six days, the titer reached 7.4 ± 0.8 mg bisabolene/L and plateaued (Fig. 6).

Interestingly, the titer increased during stationary phase and reached 22.2 ± 1.0 mg bisabolene/L at 36 days. There was no significant stripping bisabolene from the dodecane layer due to the bubbling of gas through the reactor (data not shown).

4. Discussion

Following other work to generate bisabolene from microbial cultures (Davies et al., 2014; Peralta-Yahya et al., 2011), we sought first to show that bisabolene could be produced in genetically modified *S.* 6803. The bisabolene synthase from *A. grandis* was selected as it had shown the highest activity in *E. coli* among four codon-optimized genes from species of trees (Peralta-Yahya et al., 2011). We anticipated that *S.* 6803 may have a small concentration of the precursor metabolite, farnesyl pyrophosphate (FPP), because it appears to lack a dedicated farnesyl pyrophosphate synthase. Instead, the production of FPP in *S.* 6803 likely depends on geranylgeranyl pyrophosphate synthase sometimes releasing FPP before another isopentenyl pyrophosphate reacts with FPP in the active site. Therefore, we co-expressed FPP synthase from *E. coli*, codon optimized by GenScript for expression in *S.* 6803, in an operon structure with bisabolene synthase. Transcription of this biscistronic mRNA was initiated by the tic promoter. This promoter has relatively strong expression in *S.* 6803 (Albers et al., 2015), and the presence of two lac operators maintains low expression until induced by IPTG. This was expected to be useful in the event that the expression of the two genes was toxic to *S.* 6803. We did not, however, find there to be significant impacts on growth from the expression of bisabolene synthase. The initial strain produced 1.6 ± 0.2 mg bisabolene/L after 5 days or 0.31 ± 0.04

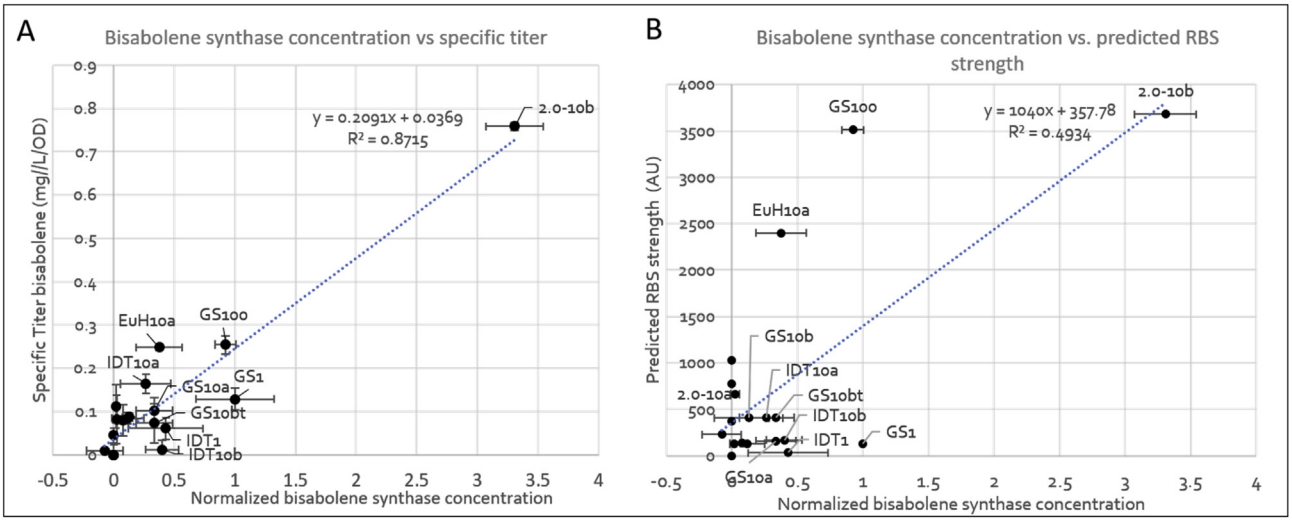

Fig. 4. Bisabolene synthase relative protein abundance measured by Western blot versus bisabolene specific titer (A) and relative measured bisabolene synthase abundance versus the RBS Calculator v2.1 predicted translation initiation rate (B). Error bars represent the standard deviation the Western blot signals from three biological replicates.

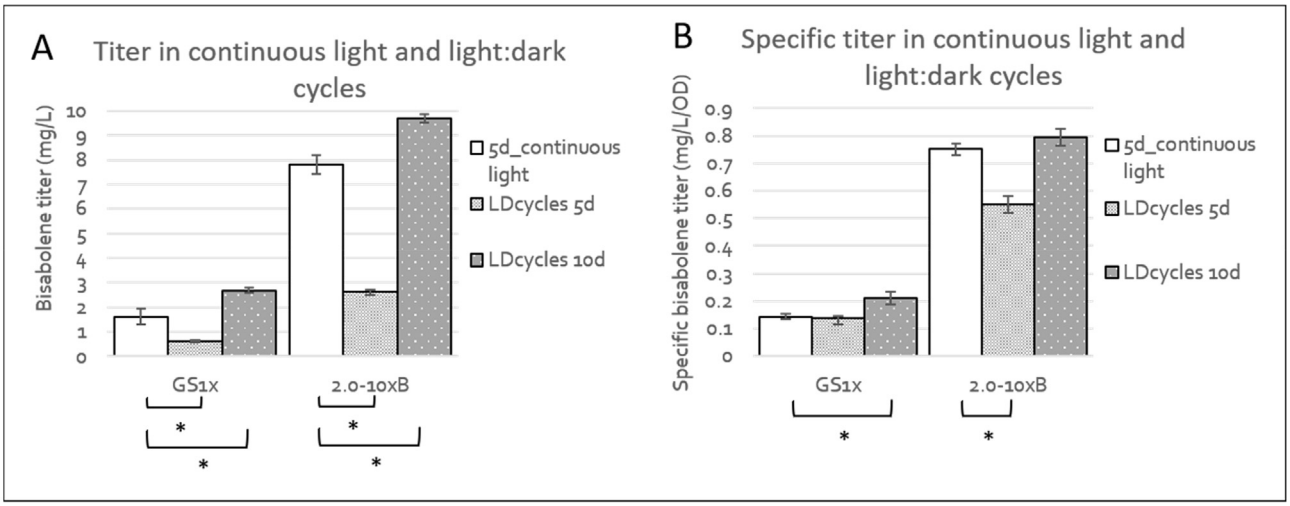

Fig. 5. Comparison of bisabolene titer and productivity for two strains grown either in continuous light (white bars) or in 12:12 light-dark cycles. Error bars indicate the standard deviation of the titer measured from three biological replicates with two GC-MS technical replicates each. Asterisks indicate significant differences titer/specific titer determined by paired *t*-test with $p < 0.05$.

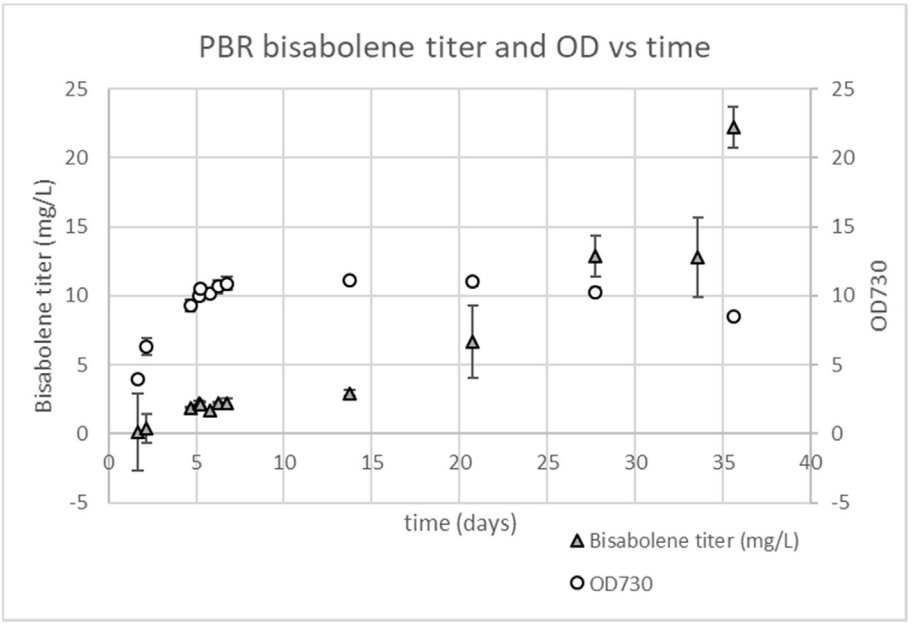

Fig. 6. (2 column widths): Bisabolene titer and growth over time in photobioreactors grown with sinusoidal light:dark cycles. Error bars indicate the standard deviation of the measurements (three biological replicates and, for titer, two technical replicates for each biological replicate).

mg/L/day, a significantly higher titer than previously reported 0.6 mg/L bisabolene titer in cyanobacteria after 4 days (Davies et al., 2014).

Building on an initial proof of concept that bisabolene synthase from *A. grandis* could be expressed and functional in *S.* 6803, we sought to increase the expression of this gene and increase the bisabolene titer achieved. Lacking a high-throughput screen for bisabolene production, we constructed a set of *S.* 6803 strains with varied codon usage (five variants) and varied RBS sequence (three or four RBS sequences for each codon usage variant).

The simple measure of CAI correlated well with bisabolene titer when compared using the same RBS. All three commercially designed gene sequences could be used to generate functional bisabolene synthase. When RBS sequences were varied, the range of bisabolene titers achieved using each of these three codon optimizations were significantly overlapping. Kudla et al. (2009) measured the fluorescence of 154 different coding sequences of gfp expressed in *E. coli* and found that the stability of mRNA secondary structure near the RBS accounted for about half of all variation in the expression level, while the CAI was a poor predictor of fluorescence (Kudla et al., 2009). This suggests that it may also be possible to improve heterologous gene expression without changing much of the sequence, and thereby avoid the requirement to synthesize the full gene sequences which may or may not be expressed at a higher level than the wild-type sequence.

The RBS sequences tested in this work show that the sequence of the 5′ untranslated region clearly impacts gene expression, but at this time we can't make accurate predictions about the expression level of a gene in *S.* 6803 based only on this sequence. The RBS Calculator poorly predicted the relative expression of bisabolene synthase in *S.* 6803. Similar results were found by Wang et al. (2018) when expressing ethylene forming enzyme in *S.* 6803. This tool was originally validated using

fluorescent protein expression in *E. coli* and, later, also in *Pseudomonas fluorescens*, *Salmonella typhimurium* LT2, and *Corynebacterium glutamicum* (Farasat et al., 2014; Salis et al., 2009). Although we do expect translation to be a similar process across species of prokaryotes, the only concession the RBS Calculator makes to differences between organisms appears to be the 16s rRNA sequence which interacts with the RBS in the mRNA. *S.* 6803 and *E. coli* have nearly identical sequences in the last 14 nucleotides at the 3′ end of their 16S rRNA and, therefore, The RBS Calculator uses the same anti-Shine-Dalgarno sequence for *S.* as it does for *E. coli* (only the final nucleotide of the 16s rRNA differs between these organisms). The translation initiation rates predicted using the RBS Calculator for the sequences used in study are generally the same or similar between the two organisms.

The ability to accurately predict relative gene expression rates would facilitate the development of more complex genetic circuits in *S.* 6803 for applications in industrial biotechnology. Genetic studies provide some evidence that translation may be different between *E. coli* and *S.* 6803. For example, a smaller proportion of genes in *S.* 6803 than in *E. coli* appear to be initiated by Shine-Dalgarno (SD) sequences (26% for *S.* 6803 versus 57% for *E. coli*) (Ma et al., 2002). It is not clear whether SD sequences should be expected to increase translation initiation rates in *S.* 6803 as much as they do in *E. coli*. SD-antiSD hybridization is thought to reduce the impact of mRNA secondary structure on translation initiation (de Smit and van Duin, 1994). However, cyanobacterial mRNA that lack SD sequences are generally predicted to have weaker secondary structure adjacent to the start codon (on either side) than the mRNAs of γ-proteobacteria that lack a SD sequence (Scharff et al., 2011). Optimal spacing between the start codon and SD sequence can also influence translation initiation rates. RBS Calculator penalizes deviation in spacing from five nucleotides between the SD and start codon (Salis et al., 2009). Ma et al. found the most frequent spacing for between SD and the start codon to be five for *E. coli*, and seven for *S.* 6803 (Ma et al., 2002).

We were also surprised that cultivation of the best performing strain in photobioreactors supplemented with CO_2 did not significantly increase the product titer beyond what was measured from shake flask cultivation. We expected these cultures to reach higher optical densities in the CO_2-rich environment and also to have higher precursor availability for bisabolene synthase. However, both the maximum optical density and the titer after five days growth were similar to what was measured from shake flask cultures. It is likely that, in both cases, a nutrient other than carbon becomes limiting and prevents further growth and bisabolene production. For example, Clark et al. (2018) increased the concentration of nitrate by more than 10-fold, the concentration of phosphate by nearly 80-fold and the concentration of iron by more than 35-fold in Media A to reach higher cell densities of *Synechococcus* sp. PCC 7002 (Clark et al., 2018).

In both shake flask and PBR cultures subjected to light:dark cycles, bisabolene titer continued to increase after the cultures reached stationary phase. The bisabolene titer in PBR cultures increased significantly after they reached stationary phase and the specific titer increased from 0.26 ± 0.03 mg/L/OD after 14 days of growth to 2.6 ± 0.19 mg/L/OD after 36 days of growth. This result suggests that the methylerythritol 4-phosphate pathway may remain active during stationary phase, and continue to make IPP, DMAPP, and FPP available for bisabolene synthesis. Carotenoid production is also reliant on the MEP pathway and may increase during the stationary phase as the cells experience low light in the high-density culture. Carotenoids also have photoprotective properties, and their increased production may also be necessary for the periods of time that the cell are exposed to the high light intensity of the surface of the culture.

These results are similar to the findings of others. In terms of the product titer, Davies et al. (2014) expressed the same DNA2.0 codon optimized bisabolene synthase sequence in *Synechococcus* sp. PCC 7002 using a *cpcBA* promoter from *S.* 6803. Their tests resulted in a bisabolene titer of 0.6 mg/L after 96 h of growth in continuous light (6 μg/L/hr). Wichmann et al. (2018) engineered strains of the algae *Chlamydomonas reinhardtii* to produce titers of 3.9 mg/L of bisabolene in phototrophic conditions and 11.0 mg/L in mixotrophic conditions after seven days of growth. Wang et al. (2018) tested a small set of RBS sequences driving expression of ethylene forming enzyme in *S.* 6803, achieving a 2.5-fold increase above the base strain.

We utilized a solvent layer of dodecane to collect produced bisabolene, following the work of others (Davies et al., 2014; Peralta-Yahya et al., 2011). The dodecane layer formed an emulsion after a few days of growth in both the shake flasks and the photobioreactors. Occasionally, samples of this emulsion required brief centrifugation in order to collect a completely organic sample. We did not find any growth inhibition due to the addition of dodecane in shake flasks and bisabolene was not detected following extraction (Bligh and Dyer, 1959) of cells harvested from cultures grown with dodecane (data not shown). Molecular dynamics models have supported the hypothesis that bisabolene may diffuse through the cell membrane into aqueous media, or, more rapidly, into dodecane in contact with the cell (Vermaas et al., 2018). Conversely, it has also been reported, in studies using *Dunaliella salina*, that a stagnant dodecane layer did not result in cell death while dodecane sparged through a culture did result in cell death (Kleinegris et al., 2011). The collection of excreted, hydrophobic, and volatile products from cyanobacterial or microalgal cultures which are grown outside to utilize sunlight is an area that requires further research into both the mechanism by which they are excreted (as this may limit the production rate), as well as into cost effective means of capturing the excreted product.

Our findings reinforce that it continues to be necessary to test combinations of genetic components in *S.* 6803 to obtain a desired outcome because present tools for predicting the effects of the components are inadequate. Combinations of RBSs and codon optimizations resulted in 3.3-fold increase in the concentration of bisabolene synthase over our original strain. However, even the highest expressing strain, bisabolene production likely remains limited by the expression of this enzyme. In this strain, 2.0–10xB, bisabolene synthase was estimated at just 0.4% of the total protein. Continued progress in metabolic engineering of cyanobacteria would benefit from improved understanding of translation initiation mechanisms in cyanobacteria and how they may differ from our understanding of translation initiation mechanisms in *E. coli*. Further improvements to genetic component design rules are needed to reduce the impacts of context dependence on the function of the components.

Declaration of competing interest

The authors declare no conflict of interest.

Acknowledgements

This work was supported by a grant from the National Science Foundation (Award #1332404). The DNA2.0 optimized bisabolene synthase gene was provided as a gift by Dr. Fiona Davies. Dr. Sei Jin Park completed LC-MS/MS analysis of 2.0-10xB proteins.

Appendix A. Supplementary data

Supplementary data to this article can be found online at https://doi.org/10.1016/j.mec.2019.e00117.

References

Albers, S.C., Gallegos, V.A., Peebles, C.A.M., 2015. Engineering of genetic control tools in Synechocystis sp. PCC 6803 using rational design techniques. J. Biotechnol. 216, 36–46. https://doi.org/10.1016/j.jbiotec.2015.09.042.

Batan, L., Quinn, J., Willson, B., Bradley, T., 2010. Net energy and greenhouse gas emission evaluation of biodiesel derived from microalgae. Environ. Sci. Technol. 44, 7975–7980. https://doi.org/10.1021/es102052y.

Bligh, E.G., Dyer, W.J., 1959. A rapid method OF total lipid extraction and purification. Can. J. Biochem. Physiol. 37, 911–917. https://doi.org/10.1139/o59-099.

Carroll, A.L., Case, A.E., Zhang, A., Atsumi, S., 2018. Metabolic engineering tools in model cyanobacteria. Metab. Eng. https://doi.org/10.1016/j.ymben.2018.03.014.

Cheah, Y.E., Albers, S.C., Peebles, C.A.M., 2013. A novel counter-selection method for markerless genetic modification in *Synechocystis* sp. PCC 6803. Biotechnol. Prog. 29, 23–30. https://doi.org/10.1002/btpr.1661.

Clark, R.L., McGinley, L.L., Purdy, H.M., Korosh, T.C., Reed, J.L., Root, T.W., Pfleger, B.F., 2018. Light-optimized growth of cyanobacterial cultures: growth phases and productivity of biomass and secreted molecules in light-limited batch growth. Metab. Eng. 47, 230–242. https://doi.org/10.1016/j.ymben.2018.03.017.

Davies, F.K., Work, V.H., Beliaev, A.S., Posewitz, M.C., 2014. Engineering limonene and bisabolene production in wild type and a glycogen-deficient mutant of Synechococcus sp. PCC 7002. Front. Bioeng. Biotechnol. 2 https://doi.org/10.3389/fbioe.2014.00021.

de Smit, M.H., van Duin, J., 1994. Translational initiation on structured messengers. Another role for the Shine-Dalgarno interaction. J. Mol. Biol. 235, 173–184.

Dismukes, G.C., Carrieri, D., Bennette, N., Ananyev, G.M., Posewitz, M.C., 2008. Aquatic phototrophs: efficient alternatives to land-based crops for biofuels. Curr. Opin. Biotechnol. 19, 235–240. https://doi.org/10.1016/j.copbio.2008.05.007.

Espah Borujeni, A., Channarasappa, A.S., Salis, H.M., 2014. Translation rate is controlled by coupled trade-offs between site accessibility, selective RNA unfolding and sliding at upstream standby sites. Nucleic Acids Res. 42, 2646–2659. https://doi.org/10.1093/nar/gkt1139.

Espah Borujeni, A., Salis, H.M., 2016. Translation initiation is controlled by RNA folding kinetics via a ribosome drafting mechanism. J. Am. Chem. Soc. https://doi.org/10.1021/jacs.6b01453.

Espah Borujeni, A., Cetnar, D., Farasat, I., Smith, A., Lundgren, N., Salis, H.M., 2017. Precise quantification of translation inhibition by mRNA structures that overlap with the ribosomal footprint in N-terminal coding sequences. Nucleic Acids Res. 45, 5437–5448. https://doi.org/10.1093/nar/gkx061.

Farasat, I., Kushwaha, M., Collens, J., Easterbrook, M., Guido, M., Salis, H.M., 2014. Efficient search, mapping, and optimization of multi-protein genetic systems in diverse bacteria. Mol. Syst. Biol. 10 https://doi.org/10.15252/msb.20134955, 731–731.

Ferreira, E.A., Pacheco, C.C., Pinto, F., Pereira, J., Lamosa, P., Oliveira, P., Kirov, B., Jaramillo, A., Tamagnini, P., 2018. Expanding the toolbox for Synechocystis sp. PCC 6803: validation of replicative vectors and characterization of a novel set of promoters. Synth. Biol. 3 https://doi.org/10.1093/synbio/ysy014.

Gao, X., Gao, F., Liu, D., Zhang, H., Nie, X., Yang, C., 2016. Engineering the methylerythritol phosphate pathway in cyanobacteria for photosynthetic isoprene production from CO $_2$. Energy Environ. Sci. 9, 1400–1411. https://doi.org/10.1039/C5EE03102H.

Gaspar, P., Oliveira, J.L., Frommlet, J., Santos, M.A.S., Moura, G., 2012. EuGene: maximizing synthetic gene design for heterologous expression. Bioinformatics 28, 2683–2684. https://doi.org/10.1093/bioinformatics/bts465.

Gibson, D.G., Young, L., Chuang, R.-Y., Venter, J.C., Hutchison, C.A., Smith, H.O., 2009. Enzymatic assembly of DNA molecules up to several hundred kilobases. Nat. Methods 6, 343–345. https://doi.org/10.1038/nmeth.1318.

Gonçalves, A.L., Rodrigues, C.M., Pires, J.C.M., Simões, M., 2016. The effect of increasing CO 2 concentrations on its capture, biomass production and wastewater bioremediation by microalgae and cyanobacteria. Algal Res. 14, 127–136. https://doi.org/10.1016/j.algal.2016.01.008.

Huang, H.H., Camsund, D., Lindblad, P., Heidorn, T., 2010. Design and characterization of molecular tools for a Synthetic Biology approach towards developing cyanobacterial biotechnology. Nucleic Acids Res. 38, 2577–2593. https://doi.org/10.1093/nar/gkq164.

Huang, H.-H., Lindblad, P., 2013. Wide-dynamic-range promoters engineered for cyanobacteria. J. Biol. Eng. 7, 10. https://doi.org/10.1186/1754-1611-7-10.

Hughes, A.R., Sulesky, A., Andersson, B., Peers, G., 2018. Sulfate amendment improves the growth and bioremediation capacity of a cyanobacteria cultured on municipal wastewater centrate. Algal Res. 32, 30–37. https://doi.org/10.1016/j.algal.2018.03.004.

Jin, H., Wang, Y., Idoine, A., Bhaya, D., 2018. Construction of a shuttle vector using an endogenous plasmid from the cyanobacterium Synechocystis sp. PCC6803. Front. Microbiol. 9 https://doi.org/10.3389/fmicb.2018.01662.

Kaneko, T., Sato, S., Kotani, H., Tanaka, A., Asamizu, E., Nakamura, Y., Miyajima, N., Hirosawa, M., Sugiura, M., Sasamoto, S., Kimura, T., Hosouchi, T., Matsuno, A., Muraki, A., Nakazaki, N., Naruo, K., Okumura, S., Shimpo, S., Takeuchi, C., Wada, T., Watanabe, A., Yamada, M., Yasuda, M., Tabata, S., 1996. Sequence analysis of the genome of the unicellular cyanobacterium Synechocystis sp. strain PCC6803. II. Sequence determination of the entire genome and assignment of potential protein-coding regions. DNA Res. Int. J. Rapid Publ. Rep. Genes Genomes 3, 109–136.

Kiyota, H., Okuda, Y., Ito, M., Hirai, M.Y., Ikeuchi, M., 2014. Engineering of cyanobacteria for the photosynthetic production of limonene from CO2. J. Biotechnol. 185, 1–7. https://doi.org/10.1016/j.jbiotec.2014.05.025.

Kleinegris, D.M.M., van Es, M.A., Janssen, M., Brandenburg, W.A., Wijffels, R.H., 2011. Phase toxicity of dodecane on the microalga Dunaliella salina. J. Appl. Phycol. 23, 949–958. https://doi.org/10.1007/s10811-010-9615-6.

Kok, S. de, Stanton, L.H., Slaby, T., Durot, M., Holmes, V.F., Patel, K.G., Platt, D., Shapland, E.B., Serber, Z., Dean, J., Newman, J.D., Chandran, S.S., 2014. Rapid and reliable DNA assembly *via* ligase cycling reaction. ACS Synth. Biol. 3, 97–106. https://doi.org/10.1021/sb4001992.

Kudla, G., Murray, A.W., Tollervey, D., Plotkin, J.B., 2009. Coding-sequence determinants of gene expression in Escherichia coli. Science 324, 255–258. https://doi.org/10.1126/science.1170160.

Lin, P.-C., Saha, R., Zhang, F., Pakrasi, H.B., 2017. Metabolic engineering of the pentose phosphate pathway for enhanced limonene production in the cyanobacterium Synechocysti s sp. PCC 6803. Sci. Rep. 7 https://doi.org/10.1038/s41598-017-17831-y.

Liu, D., Pakrasi, H.B., 2018. Exploring native genetic elements as plug-in tools for synthetic biology in the cyanobacterium Synechocystis sp. PCC 6803. Microb. Cell Factories 17. https://doi.org/10.1186/s12934-018-0897-8.

Ma, J., Campbell, A., Karlin, S., 2002. Correlations between Shine-Dalgarno sequences and gene features such as predicted expression levels and operon structures. J. Bacteriol. 184, 5733–5745.

Markley, A.L., Begemann, M.B., Clarke, R.E., Gordon, G.C., Pfleger, B.F., 2015. Synthetic biology toolbox for controlling gene expression in the cyanobacterium *Synechococcus* sp. strain PCC 7002. ACS Synth. Biol. 4, 595–603. https://doi.org/10.1021/sb500260k.

Pade, N., Hagemann, M., 2014. Salt acclimation of cyanobacteria and their application in biotechnology. Life 5, 25–49. https://doi.org/10.3390/life5010025.

Pattanaik, B., Lindberg, P., 2015. Terpenoids and their biosynthesis in cyanobacteria. Life 5, 269–293. https://doi.org/10.3390/life5010269.

Peralta-Yahya, P.P., Ouellet, M., Chan, R., Mukhopadhyay, A., Keasling, J.D., Lee, T.S., 2011. Identification and microbial production of a terpene-based advanced biofuel. Nat. Commun. 2, 483. https://doi.org/10.1038/ncomms1494.

Reinsvold, R.E., Jinkerson, R.E., Radakovits, R., Posewitz, M.C., Basu, C., 2011. The production of the sesquiterpene β-caryophyllene in a transgenic strain of the cyanobacterium synechocystis. J. Plant Physiol. 168, 848–852. https://doi.org/10.1016/j.jplph.2010.11.006.

Salis, H.M., Mirsky, E.A., Voigt, C.A., 2009. Automated design of synthetic ribosome binding sites to control protein expression. Nat. Biotechnol. 27, 946–950. https://doi.org/10.1038/nbt.1568.

Scharff, L.B., Childs, L., Walther, D., Bock, R., 2011. Local absence of secondary structure permits translation of mRNAs that lack ribosome-binding sites. PLoS Genet. 7, e1002155 https://doi.org/10.1371/journal.pgen.1002155.

Schneider, C.A., Rasband, W.S., Eliceiri, K.W., 2012. NIH Image to ImageJ: 25 years of image analysis. Nat. Methods 9, 671–675. https://doi.org/10.1038/nmeth.2089.

Sharp, P.M., Li, W.-H., 1987. The codon adaptation index-a measure of directional synonymous codon usage bias, and its potential applications. Nucleic Acids Res. 15, 1281–1295. https://doi.org/10.1093/nar/15.3.1281.

Stanier, R.Y., Deruelles, J., Rippka, R., Herdman, M., Waterbury, J.B., 1979. Generic assignments, strain histories and properties of pure cultures of cyanobacteria. Microbiology 111, 1–61. https://doi.org/10.1099/00221287-111-1-1.

Vermaas, J.V., Bentley, G.J., Beckham, G.T., Crowley, M.F., 2018. Membrane permeability of terpenoids explored with molecular simulation. J. Phys. Chem. B 122, 10349–10361. https://doi.org/10.1021/acs.jpcb.8b08688.

Wang, B., Eckert, C., Maness, P.-C., Yu, J., 2018. A genetic toolbox for modulating the expression of heterologous genes in the cyanobacterium *Synechocystis* sp. PCC 6803. ACS Synth. Biol. 7, 276–286. https://doi.org/10.1021/acssynbio.7b00297.

Werner, A., Broeckling, C.D., Prasad, A., Peebles, C.A.M., 2019. A comprehensive time-course metabolite profiling of the model cyanobacterium Synechocystis sp. PCC 6803 under diurnal light:dark cycles. Plant J. https://doi.org/10.1111/tpj.14320.

Wichmann, J., Baier, T., Wentnagel, E., Lauersen, K.J., Kruse, O., 2018. Tailored carbon partitioning for phototrophic production of (E)-α-bisabolene from the green microalga Chlamydomonas reinhardtii. Metab. Eng. 45, 211–222. https://doi.org/10.1016/j.ymben.2017.12.010.

Yu, J., Liberton, M., Cliften, P.F., Head, R.D., Jacobs, J.M., Smith, R.D., Koppenaal, D.W., Brand, J.J., Pakrasi, H.B., 2015. Synechococcus elongatus UTEX 2973, a fast growing cyanobacterial chassis for biosynthesis using light and CO2. Sci. Rep. 5 https://doi.org/10.1038/srep08132.